Modulation of electronic structures of bases through DNA recognition of protein

2010 J. Phys.: Condens. Matter 22 152101

(http://iopscience.iop.org/0953-8984/22/15/152101)

IOP FTC
IOP Publishing
Journal of Physics: Condensed Matter
J. Phys.: Condens. Matter **22** (2010) 152101 (7pp)
doi:10.1088/0953-8984/22/15/152101

FAST TRACK COMMUNICATION

Modulation of electronic structures of bases through DNA recognition of protein

Yohsuke Hagiwara[1,2], **Hiori Kino**[3] and **Masaru Tateno**[1,2,4]

[1] Center for Computational Sciences, University of Tsukuba, Tennodai 1-1-1, Tsukuba, Ibaraki, Japan
[2] Graduate School of Pure and Applied Sciences, University of Tsukuba, Tennodai 1-1-1, Tsukuba, Ibaraki, Japan
[3] Computational Materials Science Center, National Institute for Materials Science (NIMS), Sengen 1-2-1, Tsukuba, Ibaraki 305-0047, Japan

E-mail: tateno@ccs.tsukuba.ac.jp

Received 2 February 2010
Published 9 March 2010
Online at stacks.iop.org/JPhysCM/22/152101

Abstract
The effects of environmental structures on the electronic states of functional regions in a fully solvated DNA•protein complex were investigated using combined *ab initio* quantum mechanics/molecular mechanics calculations. A complex of a transcriptional factor, PU.1, and the target DNA was used for the calculations. The effects of solvent on the energies of molecular orbitals (MOs) of some DNA bases strongly correlate with the magnitude of masking of the DNA bases from the solvent by the protein. In the complex, PU.1 causes a variation in the magnitude among DNA bases by means of directly recognizing the DNA bases through hydrogen bonds and inducing structural changes of the DNA structure from the canonical one. Thus, the strong correlation found in this study is the first evidence showing the close quantitative relationship between recognition modes of DNA bases and the energy levels of the corresponding MOs. Thus, it has been revealed that the electronic state of each base is highly regulated and organized by the DNA recognition of the protein. Other biological macromolecular systems can be expected to also possess similar modulation mechanisms, suggesting that this finding provides a novel basis for the understanding for the regulation functions of biological macromolecular systems.

S Online supplementary data available from stacks.iop.org/JPhysCM/22/152101/mmedia

(Some figures in this article are in colour only in the electronic version)

1. Introduction

Electronic structures of DNA have attracted interest in several fields of science. For instance, it is well known that damage by radicals occurring on DNA bases is promoted to other sites through the charge transfer (i.e., the conductivity) of the double-helical DNA structure, suggesting that the electronic properties of DNA are important to its functions [1]. For such possible damage sites (i.e., guanine bases), DNA binding proteins can regulate the oxidation potential; for instance, Bam HI (a restriction enzyme), which binds the specific DNA core sequence, is supposed to protect the native electronic states of guanine bases from damage [2]. This suggests that protein can modulate the electronic states of DNA molecules, thereby playing a crucial role in the biological functions. Moreover, it has been reported that environmental effects of the solvent water and ions on the electronic structures of DNA are also crucial to its conductivity [3–6].

For analyses of such issues, combined *ab initio* quantum mechanics (QM)/molecular mechanics (MM) calculations have been used extensively as a useful tool [7–13], since the functional roles of the active centers and the environmental

[4] Author to whom any correspondence should be addressed.

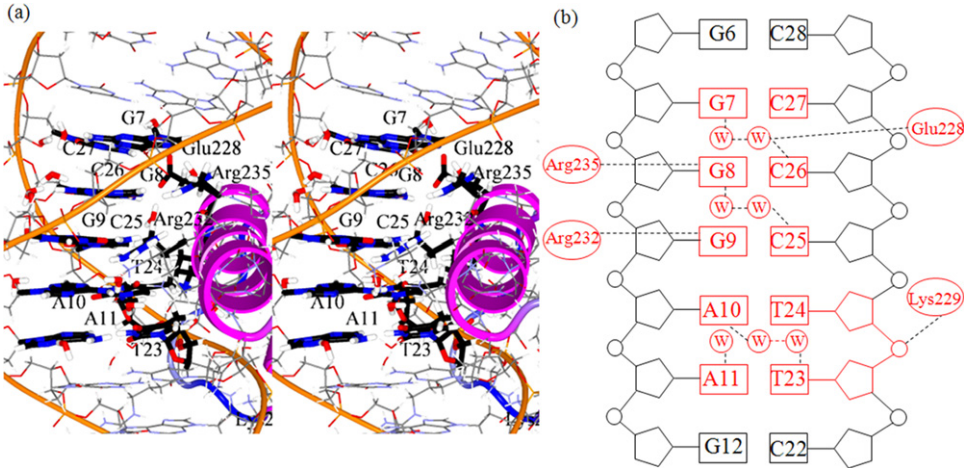

Figure 1. (a) Stereo view in the mode of recognition of DNA by PU.1. Atoms in QM and MM regions are depicted as sticks and wires, respectively. (b) Schematic representation of the mode of recognition of DNA by PU.1. W represents crystallographic water molecules. Atoms assigned as QM atoms are red. Thus, 338 atoms are included in the QM regions.

factors can be separately analyzed by using some distinct computational models [14–18]. In general, experimental techniques are restricted to investigating details of these issues, due to difficulties involved in performing separate analyses of a system for the active center and its surrounding regions. In these calculations, two distinct approaches are employed for evaluating long-range electrostatic interactions between QM and MM atoms [13]. In one scheme, partial charges of the MM atoms are involved in a QM Hamiltonian to consider the effects of the MM atoms on the electronic structures of the QM atoms (the additive scheme). In the other scheme, the effects of polarization on the electronic structure of QM atoms are ignored (the subtractive scheme). Accordingly, electronic structures and properties have been shown to be dependent on QM/MM schemes for treating partial charges of MM regions [19]. This indicates that, to address the problems arising due to the environmental effects on the active centers, we require a strict treatment of partial charges of MM atoms in a QM Hamiltonian and systematic comparisons between calculations in the presence and absence of the effects of MM partial charges.

Thus, more crucial problems, such as the mechanisms of the effects induced by the long-range electrostatic interactions, are expected to be resolved. However, as far as we know, only few studies have been reported on the influence of proteins in the electronic structures of DNA, specifically analyzed at the molecular orbital (MO) level. For this purpose, we conducted QM/MM calculations, applying various QM/MM schemes with use of our interface program to connect QM and MM engines [14, 20]. As a model system, we used a solvated structure of PU.1 in a complex with the double-stranded DNA (figure 1) [21]. PU.1 is a member of the Ets family of proteins consisting of transcriptional factors, binding with the consensus DNA sequence, 5′-GGAA-3′, as the core sequence in the DNA. In this system, catalytic reactions do not occur. Accordingly, we expect general results to be applicable to enzymatic reactions of DNA•protein complexes and other reactions without being biased towards the reactivity specific to the systems analyzed.

2. Methodology

2.1. Construction of the modeled structure

The coordinates of a crystal structure of PU.1 in a complex with the target DNA were obtained from the Protein Data Bank (PDB; PDB ID: 1PUE) [21]. Hydrogen atoms were added to the crystal structure using the LEAP module of the AMBER 9 package [22]. Then, the protein was fully solvated in spherical water droplets, in a radius of 40 Å from the center of the mass of the complex, including all crystallographic water molecules. A TIP3P water model was used for the solvation. Thus, the total atom number for the solvated protein–DNA complex system was 24 414.

To obtain energetically favorable configurations of the solvent water molecules, the following procedure was adopted, which consists of two energy minimizations and a molecular dynamics (MD) simulation. With respect to the first energy minimization by the steepest descent method, the atoms which were allowed to move freely were just solvent water molecules placed by LEAP. The protein, DNA, and all crystallographic water molecules (i.e., the coordinates of those atoms are experimentally determined) were positionally constrained (not fixed) using a harmonic potential with a force constant of 500 kcal mol^{-1} Å^{-2}. Thus, the purpose of the first energy minimization is to optimize the configuration of the water molecules placed by LEAP, while the experimentally determined coordinates (the protein, DNA, and the crystallographic water molecules) were maintained. Then, the purpose of the subsequent MD simulation is to extensively relax the configuration of the placed water molecules by adding the thermal fluctuation. For that purpose, those water molecules were also allowed to move freely as the first energy minimization, while the experimentally determined atoms (the protein, DNA, and the crystallographic waters)

were also positionally constrained. Finally, the second energy minimization by the steepest descent method was performed for obtaining the optimized structure of the system where the experimental structure was maintained while the bulk water molecules were relaxed.

It should be noted here that as a result of using the above-mentioned setup procedure for the modeled system, the crystal structure is fundamentally preserved and that one can assume the crystal structure of the complex of PU.1 and the target DNA in the present QM/MM calculations. In fact, our procedure is extensively used to obtain the energetically favorable configuration for the solvent water molecules involved in the modeled systems [14, 20, 23–26]. Further long-time MD simulations of the system in the absence of any constraints (i.e., the free dynamics) would induce conformational changes, and it is difficult to examine whether such structural transitions are really correct or not. Accordingly, in the present study, we preserved and assumed the crystal structure of the complex in the present QM/MM calculations, as mentioned. Investigations of the effects via the conformational changes of the complex are to be near future works.

All calculations were performed using the Amber 9 program package with the parm99 force field parameter. MD simulation of the solvated system was performed under a constant pressure of 1.013×10^5 Pa, with a periodic boundary condition at 300 K. Temperature and pressure were controlled by the Berendsen algorithm [27]. The SHAKE algorithm was used to treat the bonds involving hydrogen [28], and the time step for integration was set as 1 fs. Electrostatic interactions were calculated by the particle mesh Ewald (PME) method [29] with a dielectric constant 1.0. The cutoff of 12 Å was used to calculate the direct space sum for PME.

2.2. Computational details of QM/MM calculations

QM regions include the DNA core sequence, i.e., G8•C26, G9•C25, A10•T24, and A11•T23, and a base pair, G7•C27, which stacks with G8•C26. For the nucleotides in the QM regions, their phosphate and ribose moieties are not included in the QM regions, with the exception of those of T24, for which the phosphate is recognized by an amino acid residue, Lys229, of PU.1. With respect to the protein moiety, side chains of the following amino acid residues, which recognize nucleotides involved in QM regions, are also assigned as QM atoms, i.e., the two conserved arginines (Arg232 and Arg235), Glu228 (which recognizes bases of C25 and C26), and Lys229 (which recognizes the phosphate of T24). In addition, ordered water molecules forming hydrogen bonds with nucleotides and the above-mentioned amino acid residues related to the intermolecular recognition are included in the QM regions. Thus, 338 atoms are assigned as QM atoms (figure 1). All of the calculation models analyzed are summarized in table 1. For each QM/MM calculation, geometrical optimization was performed in the present study.

For the part of the QM calculations, all-electron restricted Hartree–Fock (RHF)/density functional theory (DFT) hybrid calculations were employed using the B3LYP functional with use of a 6-31G* basis set. The link atom approach was used to satisfy valence requirements where the QM/MM boundary separated covalent bonded atoms. For the calculations of electrostatic interactions between QM and MM atoms, we employed two distinct schemes, the additive and subtractive schemes (see supplementary data; S1, available at stacks.iop.org/JPhysCM/22/152101/mmedia). When the additive scheme was employed, partial charges of MM atoms within 25 Å from the center of mass of the QM region were explicitly incorporated into the one-electron integral term in the QM Hamiltonian, while in the subtractive scheme, all of the interactions between the QM and other MM atoms were calculated at MM level. The partial charges were taken from the AMBER force field.

Table 1. QM/MM schemes used and QM and MM regions assigned in the present calculations.

	Models (calculations)		
	I	II	I′
QM/MM scheme	Additive	Subtractive	Additive
DNA bases[a]	QM	QM	QM
Phosphate backbone[b]	MM	—	MM
Ordered crystal water molecules[c]	QM	QM	QM
Bulk water molecules	MM	—	—
Amino acid residues in contact with DNA[d]	QM	QM	QM
Others	MM	—	MM

[a] DNA bases included in QM regions are as follows: G7•C27, G8•C26, G9•C25, A10•T24, and A11•T23.
[b] Phosphate backbones attached to T24 are assigned as QM atoms, and others as MM atoms.
[c] Crystal water molecules in contact with some of the five DNA base pairs described above.
[d] Amino acid residues in contact with the DNA are assigned as QM atoms: Glu228, Arg232, Arg235, and Lys229.

3. Results and discussion

3.1. Evaluation of the assignment of the QM region

To evaluate the validity of excluding phosphate groups from the QM regions (i.e., phosphate atoms are assigned as the MM regions), we performed three calculations for a nucleotide/nucleoside prior to QM/MM calculations for the PU.1–DNA complex: first, for a guanosine monophosphate (GMP), all atoms are assigned to the QM region (referred to as the full QM model of GMP). Second, the phosphate group of GMP is assigned to the MM region, and the other atoms are assigned to the QM region (Model A). The additive scheme is used in this QM/MM calculation. Third, a full QM calculation is performed for a guanosine (i.e., the phosphate group of GMP is removed; Model B). The comparison of Model B and the full QM model of GMP shows that the electronic structure of HOMO-1 is perturbed by the presence/absence of the phosphate group (see supplementary data, figure S2, available at stacks.iop.org/JPhysCM/22/152101/mmedia). On the other hand, in the comparison between Model A and the full QM model of GMP, such differences of MOs are not

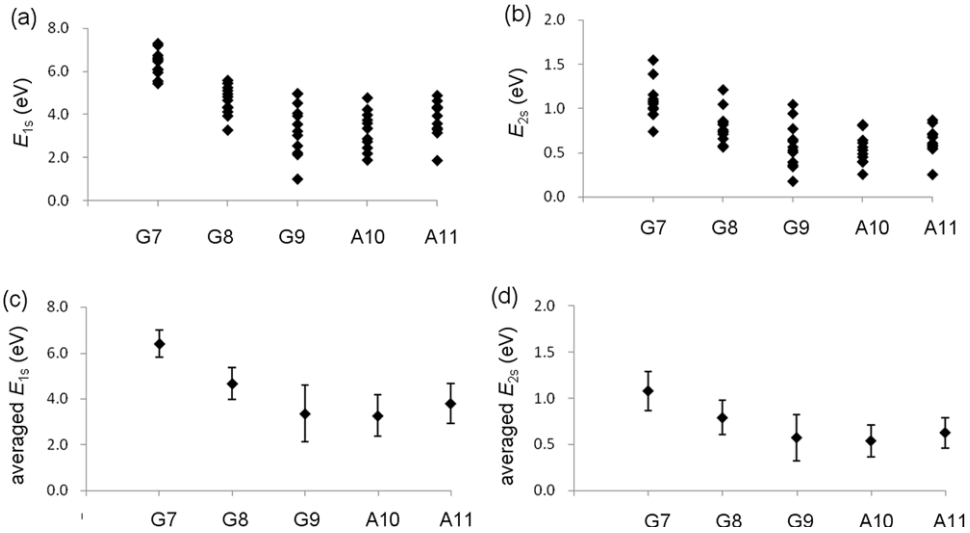

Figure 2. The effects of the MM regions (PU.1, DNA, and unordered bulk water molecules) on the electronic structures of the DNA bases (G7, G8, G9, A10, and A11) calculated using Model I. The value of E_{1s} for each atom of each base (a), that of E_{2s} (b), the averaged values of E_{1s} (c), and those of E_{2s} (d) are plotted with respect to the DNA bases. Error bars show the standard deviations of E_a values with respect to the atoms involved in a DNA base.

observed, and the orders of MOs are completely identical for those two models (see supplementary data, figure S2, available at stacks.iop.org/JPhysCM/22/152101/mmedia). These results show that the perturbation by the phosphate group is fully described by involving it as the MM region with the use of the additive scheme of our present QM/MM calculation.

3.2. Effects of PU.1, DNA, and solvent water molecules on the electronic structure

To investigate the effects of MM atoms surrounding QM regions, we first performed two calculations with distinct QM/MM schemes, referred to as Models I and II, which employ additive and subtractive schemes, respectively (table 1). With respect to each QM/MM calculation, geometrical optimization was performed in the present study. To compare the results of the two QM/MM calculations, we searched for MOs in Model I that correspond to those in Model II, on the basis of the identity of coefficients for atomic orbitals. We mapped the corresponding MOs, and found that several MOs are drastically shifted between the two models. For example, the highest occupied molecular orbital (HOMO) in Model I, which is occupied by electrons of the G7 base, corresponds to HOMO-6 in Model II, and HOMO-2 in Model II, which is localized to G9 and A10 bases, corresponds to HOMO-11 in Model I (see supplementary data, figure S3, available at stacks.iop.org/JPhysCM/22/152101/mmedia). This indicates that electronic structures of the QM region are affected by the MM regions. In our previous study, we examined various basis sets (6-31G*, 6-311G*, 6-311G**, 6-31+G*, and 6-311++G**) to investigate the effects of the MM regions on the electronic structure of the QM region, and confirmed that the effects are, in principle, independent of the basis set sizes [23]. This validates the use of 6-31G* in the following analyses.

To quantify the effects of MM regions on the electronic structures of QM regions, we have calculated one-electron integrals with respect to the partial charges of the MM atoms, i.e.,

$$E_a = \langle \chi_a | \sum_i^n \frac{q_i}{r} | \chi_a \rangle .$$

Here, q_i and n represent the partial charge of an MM atom i and the number of the MM atoms, respectively. r represents the distance between an electron and the point charge of MM atom i. χ_a represents an atomic orbital of a QM atom. In this report, we used χ_{1s} and χ_{2s}, which are atomic orbitals possessing spherical distribution. The use of 1s and 2s orbitals, each of which contains the localized electron distribution close to each atomic core, allows us to observe atomic dependence of E_a more clearly rather than using 2p orbitals which highly hybridize orbitals belonging to other atoms.

Figures 2(a) and (b) show E_a for each atom involved in the DNA bases (G7, G8, G9, A10, and A11), and figures 2(c) and (d) show the values calculated by averaging E_a for the QM atoms involved in the DNA bases. It has been revealed that the effects of the MM regions of the electronic structures are significant, e.g., the averaged E_{1s} for the G7 base is ~7.0 eV (figure 2(c)). In addition, the degrees of the deviations of the E_a values are found to also be remarkable; for example, the difference between the maximum and minimum values of E_{1s} for the atoms involved in G7 (those values are E_{1s} for the N7 atom (N represents a nitrogen atom here) and that of the N2 atom for the G7 base, respectively) is 1.9 eV (figure 2(a)).

The comparison of E_{1s} and E_{2s} shows that the trend of the environmental effects on the core orbital is common to those on the valence orbital, although the absolute values of E_{1s} are larger than those of E_{2s} because of the difference in degree of electron localization. From an experimental point of view, this diversity suggests that careful analyses might be required for experiments to seize on changes in electronic

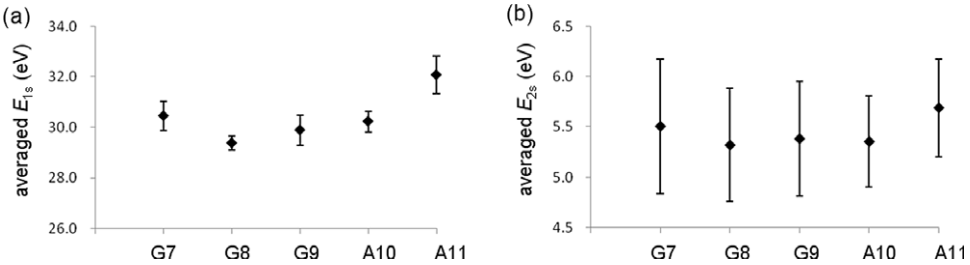

Figure 3. The effects of the MM regions (PU.1 and DNA) on the electronic structures of the DNA bases (G7, G8, G9, A10, and A11) calculated using Model I′. Perpendicular axes show the averaged values of E_{1s} (a) and E_{2s} (b) with respect to the DNA bases. Error bars show the standard deviations of E_a values with respect to the atoms involved in a DNA base.

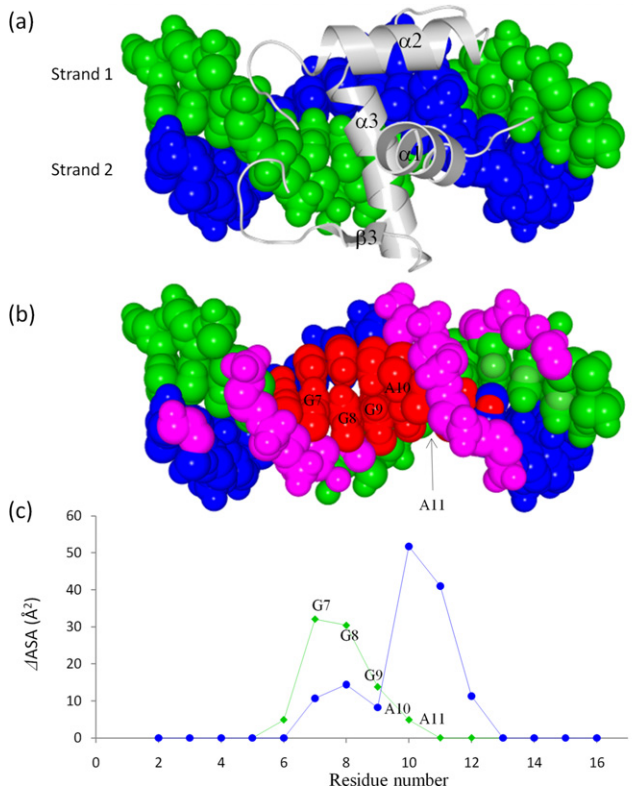

Figure 4. (a) CPK model of the DNA recognized by PU.1 in the ribbon model. Strand 1, which involves the core sequence, is colored in green, and the complementary strand, strand 2, is colored in blue. (b) The DNA regions masked by PU.1. The atoms of the DNA bases and the DNA backbone, which are located within 5 Å from the protein, are colored in red and magenta, respectively. The DNA bases (G7, G8, G9, A10, and A11) are labeled with their names. The arrow means that A11 is located behind the complementary chain. (c) The plot of ΔASA for the DNA bases. The green line and blue lines show the values for strand 1 and strand 2, respectively.

structures of DNA bases by exploiting core level energies, such as ones to measure 1s core excitations through x-ray emission spectroscopy (XES) and x-ray photoemission spectroscopy (XPS) [30].

One possible reason for the significant value with respect to the G7 base could be its position. This base is located on the QM and MM boundary; thus, it faces the MM regions directly. Accordingly, is the electronic structure of G7 sensitive to polarization by the MM atoms? However, despite A11 being also located on the QM and MM boundary, the value is not as large as that of G7. Thus, the positions of these moieties are not likely to correlate directly with the magnitude of their energy deviations induced by the electrostatic interactions of MM atoms. In other words, the difference in magnitude is not determined by the position of the QM/MM boundary. This must be explained (discussed later in this report).

3.3. Functional groups contributing to polarization

As discussed above, the E_a values allow us to evaluate the effects of MM regions composed of PU.1, the DNA, and unordered bulk water molecules. Next, to identify which functional groups in the MM regions make the main contributions to the perturbation of the electronic structure of the QM regions, we performed another calculation, referred to as Model I′ (table 1). In this calculation, the additive scheme is applied again, but all unordered bulk water molecules are removed from the system (the ordered crystal water molecules involved in QM regions of Model I are still included in Model I′). Thus, one can expect to evaluate the effects of MM regions composed of PU.1 and DNA by calculating E_a using Models I′.

The calculation shows that the effects of the protein and DNA on the electronic structures are remarkable (figure 3). Functional groups in the MM regions that make the main contributions to the significant polarization of QM regions are believed to be phosphates of the DNA, since they carry negative formal charges, −1 (the polar amino acid residue which is located in the MM region and nearest to DNA bases in the QM region is Lys245; however the distance between them is more than 10 Å apart). In fact, the E_a values obtained are positive.

The DNA base which is mostly unstabilized by the phosphate group is A11 (32.1 eV). This is particularly due to the DNA conformation which is affected by the binding of PU.1. The DNA is bent by 8° from the canonical B-DNA structure; thus, the values of a helical parameter of DNA, *twist*, for the G7, G8, G9, and A10 are approximately 30°, which are less than the twist value of the canonical B-DNA structures, 36° (see supplementary data, figure S4, available at stacks.iop.org/JPhysCM/22/152101/mmedia). On the other hand, the twist value of A11, 36.8°, is close to the canonical value. This indicates that the double helix of the DNA is rewound at the position of A11. The rewinding of the DNA

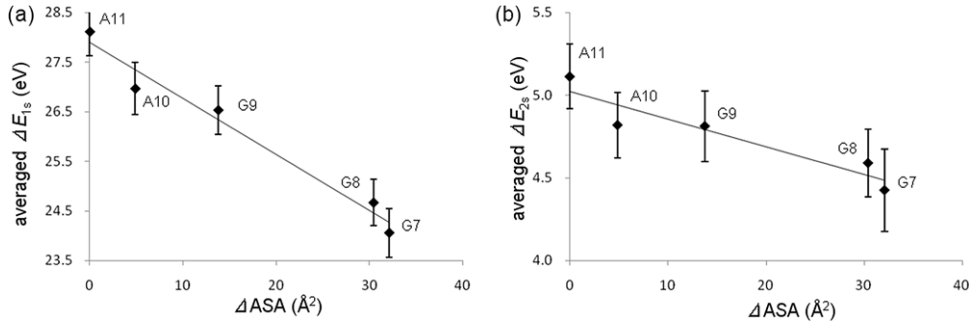

Figure 5. The effects of the MM regions (unordered bulk water) on the electronic structures of the DNA bases (G7, G8, G9, A10, and A11) calculated by subtracting E_a for Model I from E_a for Model I′, which is referred to as ΔE_a. Perpendicular axes show the averaged values of ΔE_{1s} (a) and ΔE_{2s} (b) with respect to the DNA bases. Horizontal axes show values of ΔASA for the DNA bases. Error bars show the standard deviations of ΔE_a values with respect to the atoms involved in a DNA base. The black lines in (a) and (b) are the best fit lines.

results in reducing the distance between the A11 and the phosphate groups of the complementary strand, causing the largest effects on the DNA base. Notably, comparing the E_a values with those obtained by using Model I, it is found that the E_a values for Model I are significantly smaller than those for Model I′. This indicates that bulk water molecules compensate for the increase of the E_a values via electrostatic interactions with the phosphates in the DNA. Thus, the solvent effects on the electronic structures (MO energies) are likely to significantly depend on the DNA recognition by the protein.

3.4. Solvent effects regulated by PU.1

To investigate the solvent effects in detail, we have subtracted E_a for Model I (including bulk water, PU.1, and the DNA) from E_a for Model I′ (including PU.1 and the DNA). We refer to the resultant value as ΔE_a; then, we plotted the averaged ΔE_a with respect to ΔASA. Here, ΔASA is defined as the difference between the accessible surface area (ASA) of each DNA base calculated for the DNA•PU.1 complex ($ASA_{complex}$) and the ASA calculated for the free DNA (ASA_{free}). Namely, ΔASA ($=ASA_{free} - ASA_{complex}$) represents the degree of masking of the DNA base from the solvent by the protein. Close contacts of a DNA base with amino acid residues exclude solvent water molecules surrounding the DNA base, resulting in larger ΔASA values, whereas ΔASA values are smaller when a DNA base is far from the protein (figure 4). Accordingly, the ΔASA value is expected to strongly reflect the modes of recognition of the DNA by the protein. For example, the ΔASA is calculated to be 0 $Å^2$ for A11, indicating that the base is not masked by the protein. In contrast, G7 has the largest ΔASA (32.1 $Å^2$), which indicates that the protein moiety covers the base, masking it from the solvent.

Figure 5 shows the plot of ΔASA versus averaged ΔE_a. Surprisingly, we have found a strong linear correlation between ΔASA and the effects of bulk water on the electronic structures of bases; in fact, the correlation coefficients for ΔE_{1s} and ΔE_{2s} are −0.98 and −0.94, respectively. This indicates that the electronic structures of the bases are highly modulated by the DNA•PU.1 recognition, since ΔASA for each base is significantly dependent on its binding mode. To evaluate these correlations, we used differences of Mulliken

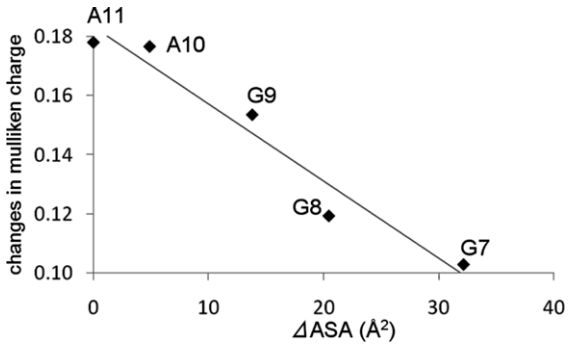

Figure 6. The close correlation between ΔASA for the DNA bases (the horizontal axis) and the absolute values of changes in Mulliken atomic charges of the bases between Models I and I′ (the perpendicular axis). The black line is the best fit line.

atomic charges on DNA bases between Models I and I′, since the magnitude of such differences represents that of the polarization induced by bulk water molecules. These changes are obtained as the absolute values of the differences between the Mulliken charges for each atom in Model I and those for the corresponding atoms in Model II. Figure 6 shows the plots of such changes in the DNA bases with respect to ΔASA. The strong correlation has been found again, as is the case with the plot of ΔE_a. This supports the presence of the above-mentioned modulation mechanism of electronic structures of DNA bases through DNA–protein recognition.

In the crystal structure of the complex, G7 is deeply inserted into the binding site of the protein; thereby, the surrounding amino acid residues exclude bulk water blocking access of water to the base (figure 7). In contrast, A11 is rather exposed to the solvent, resulting in easy access of unordered solvent water to A11. The crystal structure showed that the binding of PU.1 induces the bending of DNA with an average helical twist of 33° and an average rise per base pair of 3.2 Å [21]. As a result, the minor groove in the GGAA region is broadened by 2–3 Å from the mean value, resulting in further exposure of A11 to the solvent [21]. Thus, the effects of unordered water are significant for A11. In this manner, PU.1 determines intermolecular/interfacial contacts with target DNA, and modulates solvent-accessible surfaces on the DNA molecule in the complex. As a consequence, there are distinct

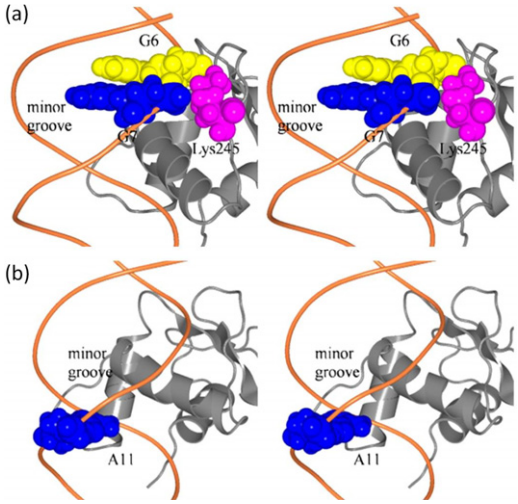

Figure 7. Stereo view of the environment surrounding (a) G7 and (b) A11. (a) The Lys245 (colored in magenta) side chain contacts with the DNA backbone of G6 and G7 (colored in yellow and blue, respectively). (b) A11 (colored in blue), in contrast, is not recognized by any amino acid residues.

responses of electronic structures of the DNA bases in the cases of G7 and A11. This could be, in general, critical to structural features/reactivity in DNA•protein complexes.

The close relationship is also expected to be useful for developing new continuum solvent models. Conventional methods, such as use of the polarized continuum model (PCM) and the conductor-like screening model (COSMO), require several parameters (for example, a set of atomic radii to define the extent of the solute) to be determined using experimental hydration free energies. It has been shown that the resultant solvation energies are strongly dependent on these radii, which would cause serious errors [31–33]. In contrast, the expected methods based on the relationship found in this study would require few parameters, e.g., coefficients of correlation of ΔE values with respect to ΔASA. The greatest advantage could be its computational cost, which is negligible when using current computers, since the additional calculation for considering the solvent effects is just the calculation of ΔASA.

4. Conclusions

The polarization effects of the regions of interest induced by the surrounding atoms may be particularly critical for investigations of, for instance, catalytic reactions occurring in enzyme•DNA complexes. The results shown in figure 5 are the first evidence to indicate the close quantitative relationship between modes of recognition of DNA bases by the protein and the electronic structures (e.g. MO energies) through the electrostatic interactions with the environment. The strong linear correlation with ΔASA and the solvation energy would be useful for an efficient calculation of solvent effects on the electronic structure; the only calculation required is computing ΔASA values (the solvation energy can be calculated by multiplying ΔASA and the correlation coefficient). The modulation mechanisms influencing the electronic structures of the active centers by regulating solvent accessibility can also be expected to occur in other biological macromolecular systems. In this manner, this can provide a novel basis for understanding mechanisms for modulation of the functions of biological macromolecular systems.

Acknowledgments

This work was partly supported by grants-in-aid from the Ministry of Education, Culture, Sports, Science and Technology (MEXT) under contract Nos 19019003 and 21340108. Computations were performed using computer facilities under the 'Interdisciplinary Computational Science Program' at the Center for Computational Sciences, University of Tsukuba, and the Computer Center for Agriculture, Forestry, and Fisheries Research, MAFF, Japan, and the Supercomputer Center, Institute for Solid State Physics, University of Tokyo.

References

[1] Merino E J, Boal A K and Barton J K 2008 *Curr. Opin. Chem. Biol.* **12** 229
[2] Nakatani K *et al* 2002 *Chem. Biol.* **9** 361
[3] Kubar T *et al* 2008 *J. Phys. Chem.* B **112** 7937
[4] Ladik J, Bende A and Bogar F 2008 *J. Chem. Phys.* **128** 105101
[5] MacNaughton J B *et al* 2006 *Phys. Rev.* B **74** 125101
[6] Solt I *et al* 2007 *J. Phys. Chem.* B **111** 6272
[7] Bruice T C 2006 *Chem. Rev.* **106** 3119
[8] Field M J *et al* 2000 *J. Comput. Chem.* **21** 1088
[9] Lin H and Truhlar D G 2007 *Theor. Chem. Acc.* **117** 185
[10] Mulholland A J 2005 *Drug. Discov. Today* **10** 1393
[11] Ryde U 2003 *Curr. Opin. Chem. Biol.* **7** 136
[12] Senn H M and Thiel W 2007 *Curr. Opin. Chem. Biol.* **11** 182
[13] Senn H M and Thiel W 2009 *Angew. Chem. Int. Edn Engl.* **48** 1198
[14] Hagiwara Y, Ohta T and Tateno M 2009 *J. Phys.: Condens. Matter* **21** 064234
[15] Jayapal P *et al* 2008 *Phys. Chem. Chem. Phys.* **10** 4249
[16] Mladenovic M *et al* 2008 *J. Am. Chem. Soc.* **130** 8696
[17] Solomon E I 2006 *Inorg. Chem.* **45** 8012
[18] Vreven T and Morokuma K 2003 *Theor. Chem. Acc.* **109** 125
[19] Murphy R B, Philipp D M and Friesner R A 2000 *J. Comput. Chem.* **21** 1442
[20] Ohta T, Hagiwara Y, Kang J, Nishikawa K, Yamamoto T, Nagao H and Tateno M 2009 *J. Comput. Theor. Nanosci.* **6** 2648
[21] Kodandapani R *et al* 1998 *Nature* **392** 630
[22] Case D A *et al* 2005 *J. Comput. Chem.* **26** 1668
[23] Kang J, Ohta T, Hagiwara Y, Nishikawa K, Yamamoto T, Nagao H and Tateno 2009 *J. Phys.: Condens. Matter* **21** 064235
[24] Hagiwara Y, Field M J, Nureki O and Tateno M 2010 *J. Am. Chem. Soc.* at press (doi:10.1021/ja9095208)
[25] Hagiwara Y, Nureki O and Tateno M 2009 *FEBS Lett.* **583** 825
[26] Hagiwara Y, Nureki O and Tateno M 2009 *FEBS Lett.* **583** 1901
[27] Berendsen H J C *et al* 1984 *J. Chem. Phys.* **81** 3684
[28] Ryckaert J P, Ciccotti G and Berendsen H J C 1977 *J. Comput. Phys.* **23** 327
[29] Darden T, York D and Pedersen L 1993 *J. Chem. Phys.* **98** 10089
[30] Harada Y *et al* 2006 *J. Phys. Chem.* A **110** 13227
[31] Klamt A *et al* 2009 *Acc. Chem. Res.* **42** 489
[32] Kongsted J, Soderhjelm P and Ryde U 2009 *J. Comput. Aided Mol. Des.* **23** 395
[33] Marenich A V *et al* 2007 *J. Chem. Theory Comput.* **3** 2011